Impact of Lateglacial cold events on the northern Aegean region reconstructed from marine and terrestrial proxy data

JQS

ULRICH KOTTHOFF,[1,2]* ANDREAS KOUTSODENDRIS,[1] JÖRG PROSS,[1] GERHARD SCHMIEDL,[2] ANDRÉ BORNEMANN,[3] CHRISTIAN KAUL,[3] GIANLUCA MARINO,[4] ODILE PEYRON[5] and RALF SCHIEBEL[6,7]
[1]Paleoenvironmental Dynamics Group, Institute of Geosciences, University of Frankfurt, Frankfurt, Germany
[2]Geological–Palaeontological Institute, University of Hamburg, Bundesstrasse 55, D-20146 Hamburg, Germany
[3]Institute of Geophysics and Geology, University of Leipzig, Leipzig, Germany
[4]Universitat Autònoma de Barcelona (UAB), Institut de Ciència i Tecnologia Ambientals (ICTA), Bellaterra, Cerdanyola del Vallès, Spain
[5]Laboratoire de Chrono-Environnement, UMR-UFC/CNRS 6249 USC INRA, University of Franche-Comté, Besançon, France
[6]National Oceanography Centre, University of Southampton, Southampton, UK
[7]University of Angers, Laboratoire des Bio-Indicateurs Actuels et fossiles, Angers, France

ABSTRACT: Marine palynomorph data paired with other indicators of sea-surface hydrography (planktic foraminiferal assemblages and oxygen isotopes) were used to decipher the impact of cold events on the northern Aegean region during the last glacial to interglacial transition. The data, which were derived from marine sediment cores GeoTü SL152 and GeoTü SL148, point to a strong impact of the Heinrich 1 and Younger Dryas cold events on surface-water conditions in the northern Aegean Sea. Shifts in marine palynomorph assemblages correlate with changes in terrestrial vegetation and climate (i.e. precipitation and temperature reconstructions based on pollen assemblages) in the northern borderlands of the Aegean Sea. The climate responses of the Aegean region to Heinrich event 1 (H1, ca. 17.5 to ca. 15.7 cal ka BP) and Younger Dryas (ca. 12.6 to ca. 11.7 cal ka BP) events appear similar in magnitude (with mean annual temperatures between ~6 and 10°C and mean annual precipitation between ~300 and ~450 mm). However, the annual temperature decline during the H1 relative to the preceding already cold conditions was minor (<3°C). The transition from the relatively warm and humid local equivalent of the Allerød interstadial to the Younger Dryas, on the other hand, witnessed an annual temperature decline of 6°C and an annual precipitation decrease of 300 mm, the latter occurring abruptly within only ca. 150 a. The return to warmer conditions in the northern Aegean region after the Younger Dryas was completed at ca. 11.6 cal ka BP. Copyright © 2011 John Wiley & Sons, Ltd.

KEYWORDS: land–sea correlation; temperature changes; Heinrich event 1; Younger Dryas; Lateglacial; eastern Mediterranean.

Introduction

Marking the transition from glacial to present-day interglacial conditions, the late Pleniglacial/Lateglacial interval (coeval with late Marine Isotope Stage 2) was punctuated by a series of millennial-scale climate oscillations that affected the ocean–atmosphere system on an interhemispheric scale (e.g. Waelbroeck et al., 2001; Barker et al., 2009). In the Northern Hemisphere, the Last Glacial Maximum was followed by a severe cold interval (i.e. Heinrich event 1 (H1), ca. 17 to ca. 15 ka ago, e.g. Bond et al., 1993), an abrupt shift to warmer conditions connected to the Bølling (ca. 14.5 to ca. 13.8 ka ago, synonymous with the 'Meiendorf interstadial' in central Western Europe; e.g. Litt et al., 2001) and Allerød interstadials (ca. 13.7 to ca. 11.7 ka ago), and a return to cold conditions during the Younger Dryas (YD, also regarded as event GS 1 in Greenland ice cores; ca. 12.7 to ca. 11.7 ka ago; e.g. Björck et al., 1998; Lowe et al., 2008). The latter oscillation precedes the final transition to the interglacial conditions of the early Holocene.

H1 and the YD had a significantly stronger impact and lasted much longer than the climate deteriorations punctuating the Holocene (Broecker, 2000). This has been shown by a number of climate records from different archives, such as ice core data from Greenland (e.g. Björck et al., 1998), lake sediment records from western Europe (Litt et al., 2001; Brauer et al., 2008), marine sediment cores from the Atlantic Ocean (e.g. Waelbroeck et al., 2001), the western Mediterranean (e.g. Cacho et al., 1999) and western Africa (Weldeab et al., 2007; Mulitza et al., 2008), and speleothem data from Asia Minor (Fleitmann et al., 2009).

H1 and the YD are probably related to a decrease in oceanic heat transport to the northern high latitudes as a result of enhanced freshwater influx to the North Atlantic (e.g. Bond et al., 1993; McManus et al., 2004; Broecker, 2006). Both the H1 and YD events show durations of the same order of magnitude (ca. 1.2 to ca. 2.0 ka), which distinguishes them from other, shorter-termed cold events during the late Pleniglacial and Lateglacial (e.g. the Oldest and Older Dryas). However, while the H1 event occurred under glacial boundary conditions, the YD interrupted an interval of near-interglacial climate, pre-dating the last summer insolation maximum of the Northern Hemisphere by merely ca. 1.5 ka (at ca. 11 ka ago; e.g. Berger and Loutre, 1991).

The eastern Mediterranean region represents an ideal area to study and compare the impacts of these climate events. It has been repeatedly demonstrated that the Aegean region reacts sensitively to short-term and muted episodes of climate change under the interglacial boundary conditions of the Holocene (e.g. Rohling et al., 2002; Kotthoff et al., 2008a,b; Pross et al., 2009; Marino et al., 2009). Furthermore, the Aegean Sea is an important region for deep-water formation, and climate changes in the Aegean region affect the thermohaline circulation in the entire eastern Mediterranean Sea (e.g. Theocharis et al., 1999; Marino et al., 2007).

To date, several records from the Aegean Sea and its borderlands (e.g. Aksu et al., 1995; Lawson et al., 2005) have allowed analysis of the regional expression of the YD to some degree. However, many of these records lack robust

*Correspondence: U. Kotthoff, [2]Geological–Palaeontological Institute, as above.
E-mail: ulrich.kotthoff@uni-hamburg.de

chronologies (see Rossignol-Strick, 1995; Kotthoff *et al.*, 2008b), which hampers the unequivocal identification of the YD. Sedimentological, micropalaeontological and palynological records from the northern Aegean Sea indicate that the YD had a strong impact on the marine and terrestrial environments in this area (Aksu *et al.*, 1995; Ehrmann *et al.*, 2007; Kuhnt *et al.*, 2007; Kotthoff *et al.*, 2008a). In the marine realm, the intermediate and deep-water formation was strengthened due to the return to colder conditions (e.g. Kuhnt *et al.*, 2007), while in the terrestrial realm the YD caused a rapid decline in forest cover and an increase in steppe elements between ca. 12.7 and ca. 11.7 cal ka BP (Kotthoff *et al.*, 2008a).

In contrast, the impact of the H1 event on terrestrial and marine environments of the Aegean region has yet remained poorly constrained; in particular, there is a lack of climate data for the terrestrial realm during the H1 interval. Investigations based on marine sediments have suggested that the H1 did not significantly affect the northern Aegean region (Hamann *et al.*, 2008). This finding appears difficult to reconcile with the evidence that even the relatively low-amplitude climate fluctuations of the Holocene left a clear imprint on terrestrial and marine environments of the Aegean region (e.g. Rohling *et al.*, 2002; Kotthoff *et al.*, 2008a,b; Pross *et al.*, 2009; Marino *et al.*, 2009).

In light of the above, we here present new organic-walled dinoflagellate cyst and oxygen isotope data in combination with previously published pollen data (Kotthoff *et al.*, 2008a) from marine core SL152 (northern Aegean Sea), integrated with new planktic foraminifer census count and previously published oxygen isotope data from neighbouring core SL148. The pollen data from core SL152 have been complemented by not yet published quantitative reconstructions for annual precipitation and temperature. Our multi-proxy approach yields a comprehensive view of the impact of late Pleniglacial and Lateglacial climatic events, notably the H1 and the YD, on terrestrial and marine ecosystems in this climatically highly sensitive region.

Regional setting

The Aegean Sea is semi-isolated from the rest of the Mediterranean Sea and characterised by a complex bathymetry, with large shelf areas in the north and northeast (Fig. 1; Perissoratis and Conispoliatis, 2003). In the south, it is connected to the Levantine and Ionian seas through several seaways. In the northeast there is a connection to the Black Sea via the Dardanelles, the Sea of Marmara and the Bosporus (Fig. 1).

The present-day wind field in the Aegean region is characterised by northerly directions, with cold and dry Arctic/polar outbreaks during winter and spring months (Poulos *et al.*, 1997; Fig. 1). In comparison to the sediment supply by rivers, aeolian sediment influx is quantitatively negligible (Chester *et al.*, 1977; Ehrmann *et al.*, 2007). Significant suspension loads are carried into the Aegean Sea by several rivers, notably from its northern borderlands (Ehrmann *et al.*, 2007; Kotthoff *et al.*, 2008b; Fig. 1); to a lesser extent, riverine input of terrigenous material is derived from western Asia Minor, e.g. via the Kara Menderes and Gediz rivers. Outflow of Black Sea surface water represents an additional source for suspended terrigenous material (e.g. Lane-Serff *et al.*, 1997; Çatağay *et al.*, 2000). According to Sperling *et al.* (2003), the connection of the Aegean Sea and the Sea of Marmara was probably already established at ca. 14 cal ka BP, and Verleye *et al.* (2009) date the establishment of a connection between the Black Sea and Sea of Marmara at ca. 8.2 cal ka BP. In any case, it was probably not until ca. 6.5 cal ka BP that the marine connection between the Aegean and Black Seas was fully established (Sperling *et al.*, 2003; Ehrmann *et al.*, 2007). The present-day outflow of Black Sea surface water into the Aegean Sea amounts to ca. $400 \, km^3 \, a^{-1}$, with highest values during the late spring and summer months (Aksu *et al.*, 1995). Surface-water temperature and salinity values in the Aegean Sea show a pronounced NE–SW gradient, with lower values in the North (Aksu et al., 1995).

Material and methods

Cores GeoTü SL152 (40° 05.19′ N, 24° 36.65′ E, water depth 978 m) and GeoTü SL148 (39° 45.23′ N, 24° 05.78′, water depth 1094 m) have been retrieved in 2001 during RV *Meteor* cruise M51/3 from the Mount Athos Basin, northern Aegean Sea, ~200 km SE of Thessaloniki (Fig. 1). The two sites are very close to one another, with the distance amounting to ~50 km.
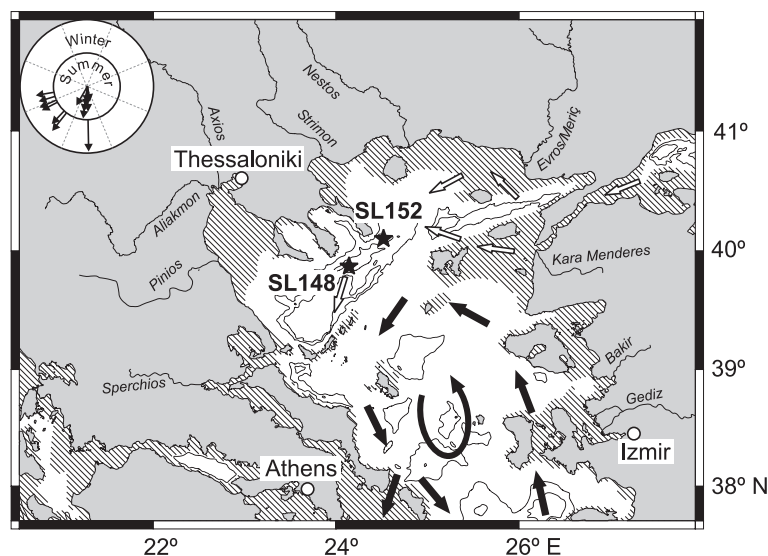

Figure 1. Map of the Aegean region. Black stars mark the locations of cores GeoTü SL152 and SL148. Hatched area indicates shelf exposed between ca. 19 and ca. 15 cal ka BP (after Cramp *et al.*, 1988; Aksu *et al.*, 1995; Perissoratis and Conispoliatis, 2003), isolines show water depths of 600 and 1000 m. White arrows indicate low-salinity Black Sea surface water flow, black arrows indicate warm and high-salinity surface water circulation, following Aksu *et al.* (1995), Lykousis *et al.* (2002) and Ehrmann *et al.* (2007). Wind directions (following May, 1982, and Poulos *et al.*, 1997) over the Aegean region during summer and winter are indicated at the top left.

Here we present centennial-scale resolution (ca. 150 a) dinocyst and planktic foraminiferal oxygen isotope data, and quantitative pollen-based terrestrial climate data from core GeoTü SL152 (SL152) comprising the time interval from ca. 19 to ca. 9 cal ka BP. These data are integrated with planktic foraminiferal census counts and oxygen isotope data from core GeoTü SL148 (temporal resolution: ca. 300 a). The selected time interval comprises the late Pleniglacial to the earliest Holocene. In-depth information on the terrestrial palynomorph assemblages and sedimentology of core SL152 has been previously provided by Kotthoff et al. (2008a,b). Detailed information on the sedimentary characteristics and benthic foraminiferal assemblages from core SL148 is given by Ehrmann et al. (2007) and Kuhnt et al. (2007).

Age model

The chronology of core SL152 is based on eight ^{14}C accelerator mass spectrometry dates obtained from *Globigerinoides ruber* (white) and, in case not enough *G. ruber* material was available, from *Globigerina bulloides*, other surface-dwelling foraminifera and pteropods. Detailed information on the age model of core SL152 is given in Kotthoff et al. (2008a,b). Three ^{14}C dates for core SL148 were obtained from *G. ruber*, *G. bulloides*, *Globigerinoides sacculifer*, *Neoglobo-quadrina incompta* and *Turborotalita quinqueloba*. Details on the age model of core SL148 are provided by Ehrmann et al. (2007). For both cores, local reservoir age corrections were applied following Siani et al. (2001; generally 400 a), and conversions to calendar ages were carried out via the radiocarbon calibration software of Fairbanks et al. (2005). Both age models have been shown to be internally consistent (Kotthoff et al., 2008a,b; Fig. 2).
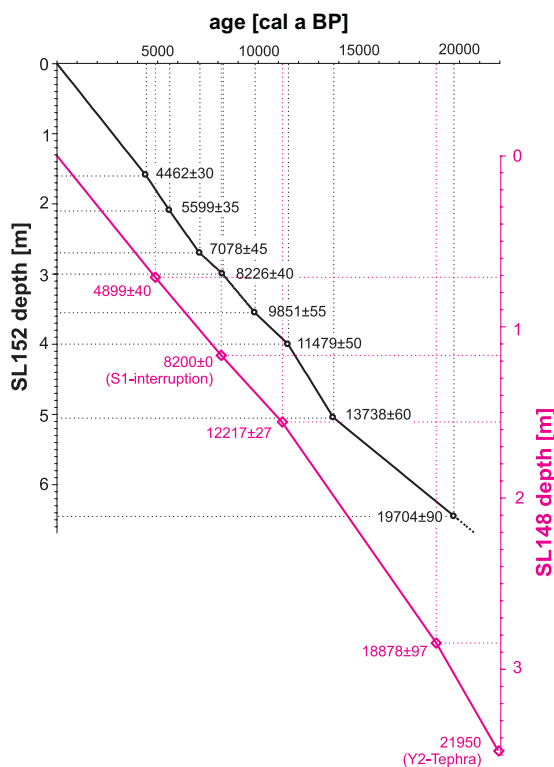
Figure 2. Comparison of the age models of core GeoTü SL152 (Kotthoff et al., 2008a) and core GeoTü SL148 (Kuhnt et al., 2007). In both cases, the ages are reservoir-corrected (following Siani et al., 2001) and converted to calendar ages (via the radiocarbon calibration software of Fairbanks et al., 2005). This figure is available in colour online at wileyonlinelibrary.com.

Analyses from core SL152

Palynomorphs

For the analysis of terrestrial and marine palynomorph assemblages, samples were taken from the interval between 6.30 and 3.27 m at a resolution of 1 cm within the sapropelic interval of core SL152. Below the interval of sapropel S1 (S1) (equivalent to ca. 9.6 to ca. 7 cal ka BP; see Kotthoff et al., 2008b), the sample spacing was either 5 or 10 cm. For the time interval discussed here (i.e. 19–9 cal ka BP), an average temporal resolution of 150 a was achieved. Per sample, 1–6 g of sediment was processed using standard palynological techniques (e.g. Pross, 2001).

Whenever possible, at least 300 terrestrial palynomorphs (excluding bisaccate pollen and spores) were determined and counted per sample. Since bisaccate pollen is generally overrepresented in marine pollen assemblages due to its particularly good transport properties and high resistance to oxidation (e.g. Rossignol-Strick and Paterne, 1999), it was excluded from the pollen sums. In general, ~200 (at least 150) organic-walled dinoflagellate cysts (dinocysts) were determined per sample.

Pollen-based quantitative climate reconstructions

To support the qualitative pollen-derived climate information, the mean annual temperature (MT_{year}) and mean annual precipitation (MP_{year}) were calculated from pollen data using the modern analogue technique (MAT; e.g. Guiot, 1990). Originally developed for continental pollen records, the MAT has been successfully applied to marine pollen assemblages (e.g. Sánchez Goñi et al., 2005; Dormoy et al., 2009; Combourieu-Nebout et al., 2009). The MAT reconstructions are based on a database with 2748 modern pollen spectra from Europe (Bordon et al., 2009), updated to 3530 by the addition of modern spectra from the Mediterranean area (Dormoy et al., 2009). Here we used the 10 modern assemblages with smallest chord distances for the reconstructions of the climate parameters. Because of its overrepresentation in marine pollen assemblages, bisaccate pollen was removed from the evaluated samples and the database (see also above).

Stable isotopes

Forty-four samples from core SL 152 were analysed for planktic foraminiferal oxygen isotope ratios. In 25 samples, the summer-mixed–layer-dwelling *Globigerinoides ruber* (white) was measured. Owing to the low abundance of *G. ruber* in the late Pleniglacial and Lateglacial sediments of core SL152, the sub-thermocline-dwelling *Neogloboquadrina incompta* was additionally used for the time interval from 17 to 12 cal ka BP (Fig. 5C).

Samples for planktic foraminifera were wet-sieved over a 63 μm mesh with tap water. *N. incompta* and *G. ruber* were hand-picked from the >150 μm fraction. Specimens were cleaned with deionised water and ultrasound for 3 s. Isotope analyses were carried out on batches of 5–10 specimens on a PDZ Europa Geo 20-20 mass spectrometer with individual acid bath carbonate preparation (orthophosphoric acid reaction at 70°C), at the National Oceanography Centre, Southampton. Isotope ratios are expressed relative to Vienna PeeDee Belemnite (VPDB). External precision is better than 0.06‰ for both δ^{13}C and δ^{18}O. Further samples (*N. incompta*) from the late Pleniglacial and Lateglacial (Fig. 5C) were measured at the Institute of Geosciences, Frankfurt University, using a Flash-EA 1112 connected to the gas source mass spectrometer MAT 253

(both Thermo-Finnigan). For these results, the external precision is better than 0.06 ‰ for δ^{13}C and 0.08 ‰ for δ^{18}O.

Analyses from core SL 148

Planktic foraminiferal assemblages

From core SL148, 35 samples covering the interval between 2.85 and 1.275 m depth have been studied for their content in planktic foraminifera. Samples were usually taken at 5 cm distance, which yields a temporal resolution between ca. 200 and ca. 400 a. The four uppermost samples (1.38–1.275 m depth) were taken at 2–2.5 cm distance. Sediment samples were dried, weighed and washed through a 63 μm screen. The determination of planktic foraminifers was carried out on the size fraction >125 μm. At least 300 specimens were counted per sample.

We distinguished between tropical/subtropical (i.e. warm-water), temperate/transitional and polar/subpolar (i.e. cold-water) assemblages following Bé and Tolderlund (1971), Hilbrecht (1996) and Kucera (2007). The warm-water assemblage is dominated by *Globigerinoides ruber* (white), *G. sacculifer*, *Globoturborotalita* spp., *Orbulina universa* and *G. ruber* (pink; in descending order of abundance, Figs 4 and 5B). The temperate/transitional assemblage is dominated by *G. bulloides*. The polar/subpolar assemblage comprises mainly *N. incompta* (cf. Darling *et al.*, 2006), *Turborotalita quinque-loba* and *N. pachyderma*. Of these forms, *N. pachyderma* prefers the coolest conditions (Hemleben *et al.*, 1989; Hilbrecht, 1996, 1997; Kucera, 2007). *T. quinqueloba* is more frequent at lower sea-surface temperatures than *N. incompta* (Hilbrecht, 1996; Kucera, 2007).

Results and discussion

Palynomorph preservation

As shown by previous studies, selective degradation affected the palynomorph assemblages from the Aegean Sea, and notably from the Mount Athos Basin, to a much lesser extent than commonly encountered in sediments from the Mediterranean Sea (compare Zonneveld *et al.*, 2001). This is due to the relatively high (>30 cm ka^{-1}) sedimentation rates in the Mount Athos basin (Kotthoff *et al.*, 2008a,b).

This view is corroborated by the distribution of dinocysts within core SL152, notably the continuous occurrence of the rather oxidation-resistant taxon *Impagidinium aculeatum* (Sangiorgi *et al.*, 2003) prior to and during S1 deposition. If selective degradation had seriously affected the dinocyst assemblages, *I. aculeatum* should exhibit increased percentages before S1 and during S1 interruptions, as has been found, for example, in the Adriatic Sea (Sangiorgi *et al.*, 2003). Instead, changes in *I. aculeatum* percentages do not vary in direct response to the deposition of sapropelic sediments. The determination coefficient between sediment lightness, which can be used as a total organic carbon (C$_{org}$) proxy and a means to differentiate between sapropelic and non-sapropelic sediments (see discussion in Kotthoff *et al.* 2008b), and the percentages of *Impagidinium* is indeed very low ($R^2 = 0.0238$, $N = 66$).
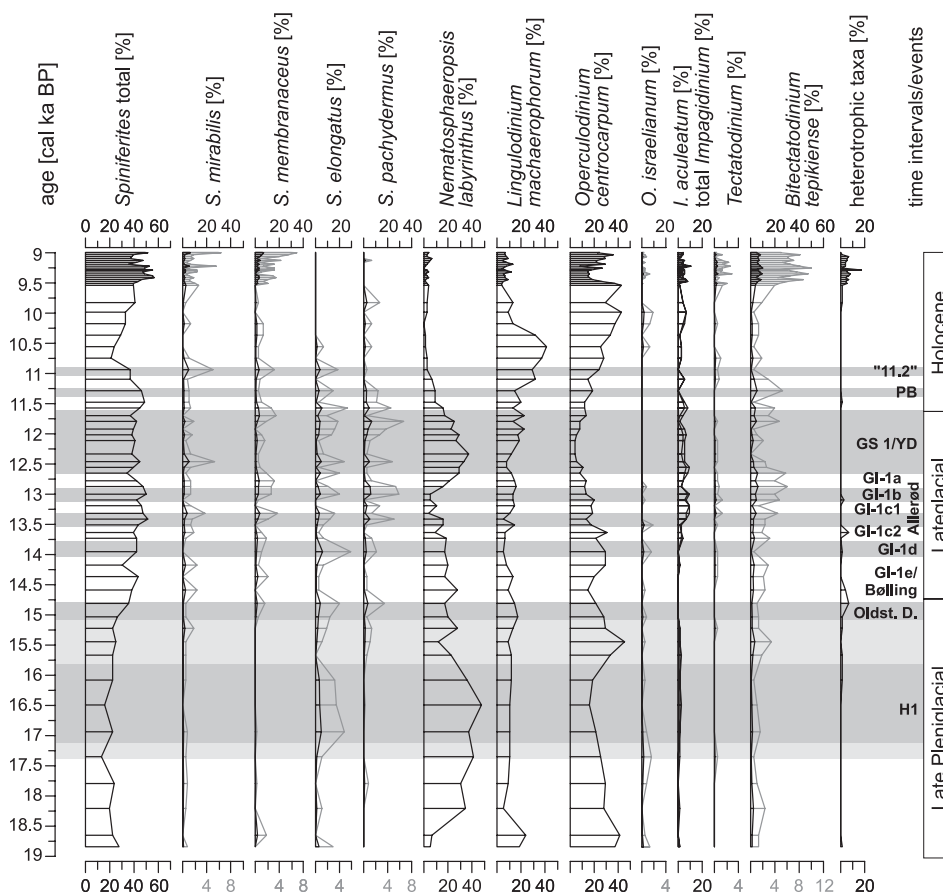
Figure 3. Relative dinocyst abundances in core SL152 vs. age. Grey bars indicate cooling events as indicated in Greenland ice cores and terrestrial proxies from core SL152 (Fig. 5; Kotthoff *et al.*, 2008a). 11.2, 11.2 ka event; PB, preboreal oscillation; GS 1/YD, Greenland stadial 1/Younger Dryas; GI, Greenland interstadial; Oldst. D., Oldest Dryas; H1, Heinrich event 1.
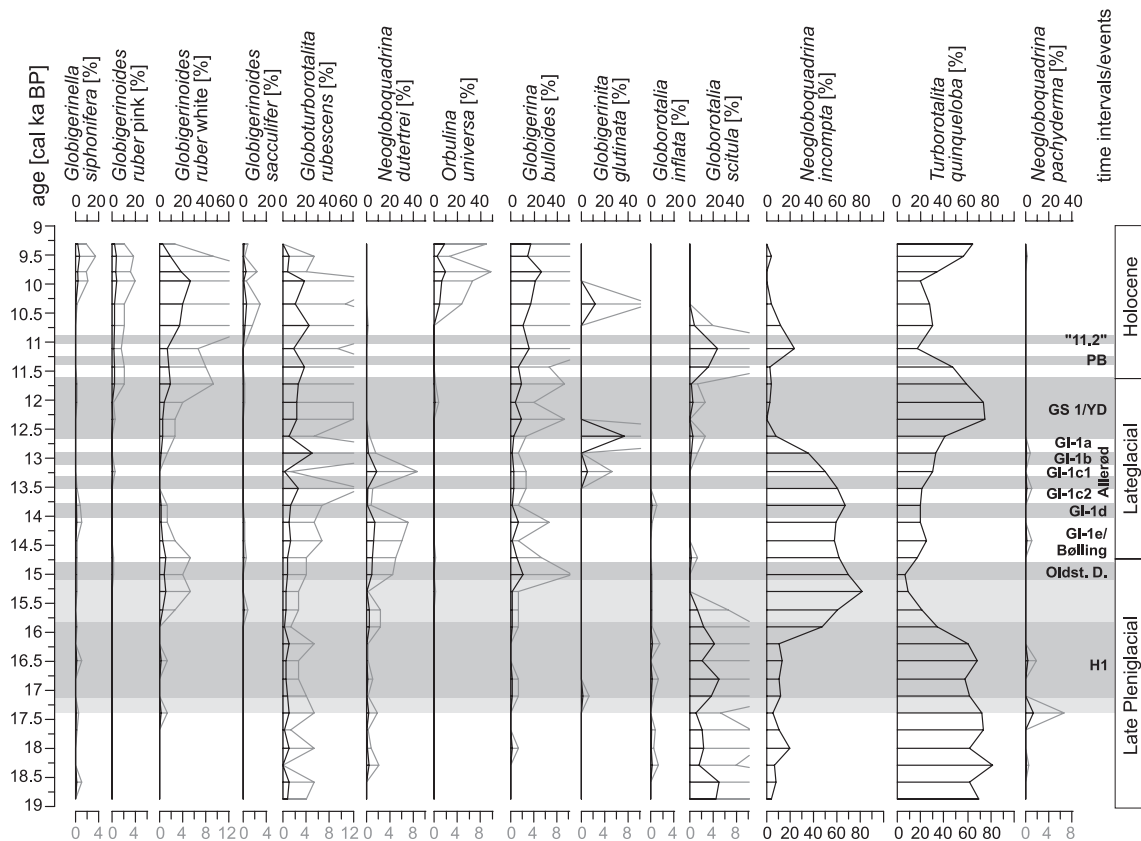
Figure 4. Relative planctic foraminifer abundances in core SL148 vs. age. Grey bars indicate cooling events as indicated in Greenland ice cores and terrestrial proxies from core SL152 (Fig. 5; Kotthoff *et al.*, 2008a). 11.2, 11.2 ka event; PB, preboreal oscillation; GS 1/YD, Greenland stadial 1/Younger Dryas; GI, Greenland interstadial; Oldst. D., Oldest Dryas; H1, Heinrich event 1.

Heterotrophic dinocyst taxa (e.g. *Brigantedinium* spp.), often considered particularly sensitive to oxidation (e.g. Zonneveld *et al.*, 2001), show a pronounced abundance increase between ca. 9.8 and ca. 9.5 cal ka BP, which roughly coincides with the onset of S1 (Fig. 3). Hence it could be argued that this abundance pattern reflects the reduced oxidation potential connected to sapropel formation. However, heterotrophic taxa also show almost sapropel-like percentages during the warm phases of the Bølling and Allerød (Fig. 3), which to our knowledge have not been featured by reduced bottom-water ventilation in the eastern Mediterranean. Thus the high percentages of heterotrophic taxa during the formation of S1 primarily reflect changes in surface-water conditions such as enhanced nutrient supply rather than enhanced preservation (see Combourieu-Nebout *et al.*, 1998; Sluijs *et al.*, 2005).

Terrestrial palynomorphs and quantitative climate reconstructions

For the interval from ca. 19 to ca. 17.5 cal ka BP, the pollen data from core SL152 suggest cooler and drier conditions in the borderlands of the northern Aegean Sea as compared to present-day conditions. This is qualitatively indicated by relatively high percentages (20–25%) of steppe element pollen (SEP). Quantitative pollen-based climate reconstructions suggest low annual terrestrial temperatures and precipitation ($MT_{year} = \sim 10°C$, $MP_{year} = \sim 450$ mm). The MT_{year} as reconstructed for the terrestrial realm is in accordance with the results of Hayes *et al.* (2005), who calculated Aegean Sea surface-water temperatures of $\sim 11°C$ for that time interval by using artificial neural networks on planktic foraminiferal assemblages.

After 17.5 cal ka BP, the decrease in non-saccate arboreal pollen (NSAP) percentages is paralleled by an MT_{year} drop of at least 1.5°C (Fig. 5F). This is followed by an increase in SEP percentages at ca. 16.5 cal ka BP and a decrease in MP_{year} (~ 100 mm a^{-1}; Fig. 5E and G). The MT_{year} remains relatively low until ca. 15 cal ka BP. From ca. 15 to ca. 12.7 cal ka BP, NSAP percentages increase to ~ 40%. The time interval from ca. 15 to ca. 12.7 cal ka BP is correlative with the tripartite Bølling/Allerød interval described from Greenland ice cores (cf. Björck *et al.*, 1998; Kotthoff *et al.*, 2008a), respectively. Minor relative increases in NSAP (at ca. 14.5, ca. 13.7, ca. 13.5 and ca. 12.8 cal ka BP), indicating more humid conditions, correlate well with the Greenland interstadials GI-1e, -1c3, -1c1 and -1a. Our pollen-based quantitative data reveal significantly higher MT_{year} and MP_{year} during that time than during the preceding late Pleniglacial. There are, however, MT_{year} and MP_{year} setbacks.

The following YD is characterised by very high percentages of SEP (up to ~ 40%). The reconstructed values for the MT_{year} and MP_{year} are even lower than during the late Pleniglacial ($\sim 6°C$ and ~ 300 mm; Fig. 5).

After the YD, the MT_{year} increases rapidly, reaching values typical of the Holocene ($\sim 13°C$) already at ca. 11.6 cal ka BP. In the pollen assemblages from core SL152, this warming is paralleled by a rapid decline in SEP percentages. The MP_{year} increases to ~ 600 mm after the YD and fluctuates around this level until ca. 10.5 cal ka BP. From ca. 10.5 until ca. 9.6 cal ka BP, it increases by another 200 mm. The general trend towards more humid conditions between ca. 11.7 and ca. 9.5 cal ka BP was interrupted by minor setbacks reflected by relatively low NSAP percentages and MP_{year} and MT_{year} decreases at ca. 11 and ca. 10.4 cal ka BP (Fig. 5).
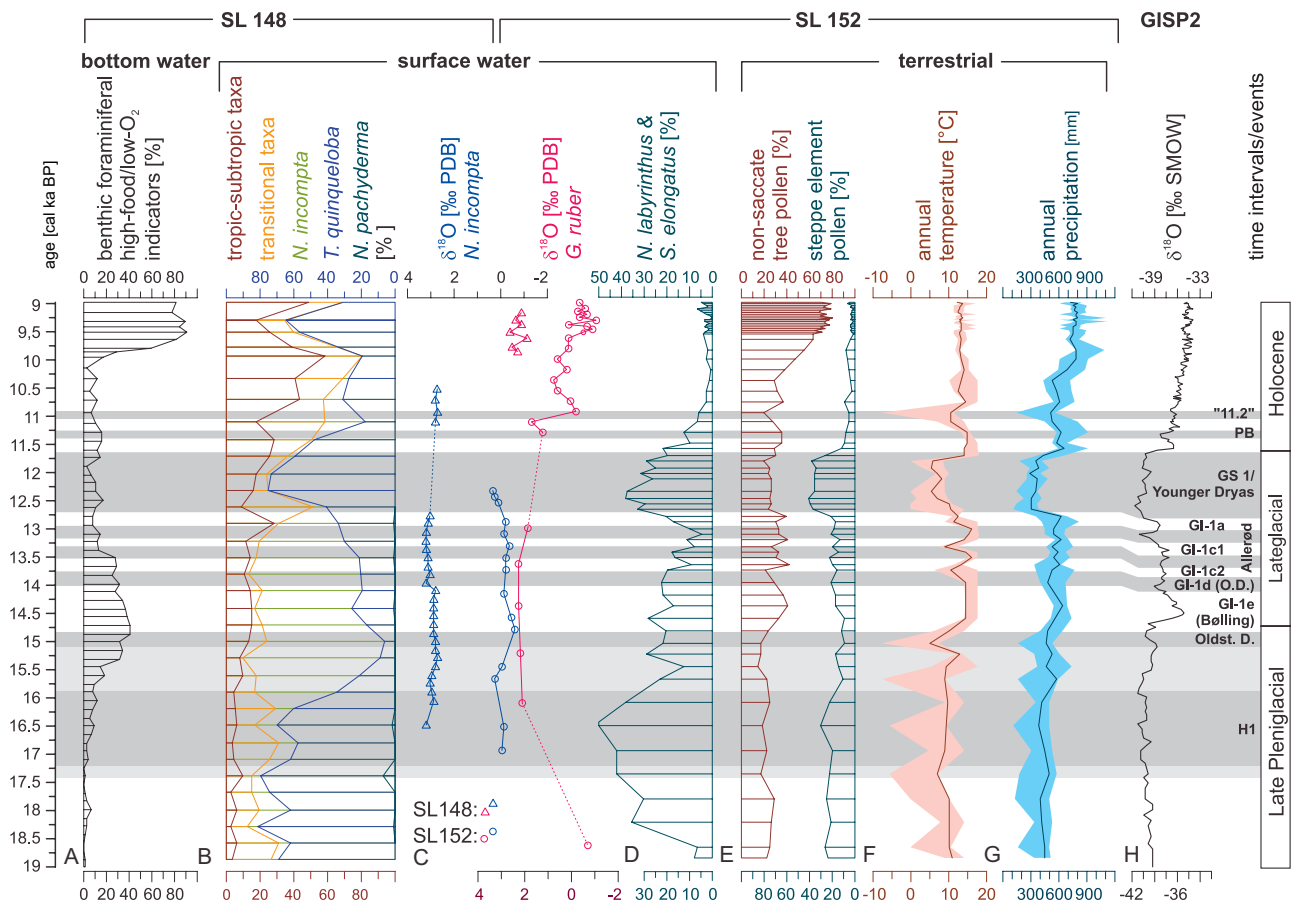
Figure 5. Biological and geochemical proxies in cores SL152 and SL148 compared to Greenland ice core data. From left to right: benthic (A) and planktic foraminifer abundances (B) and δ¹⁸O record for *Globigerinoides ruber* from core SL148 (C, triangles, Kuhnt *et al.*, 2007); δ¹⁸O records for *Globigerinoides ruber* and *Neogloboquadrina incompta* (C, circles), combined abundances of coldwater indicators *Nematosphaeropsis labyrinthus* and *Spiniferites elongatus* (D), percentages of nonsaccate tree pollen vs. percentages of steppe element pollen (E), and reconstructed (pollen-based) annual temperature (F) and annual precipitation (G) from core SL152; δ¹⁸O record from GISP2 ice core (I; http://lnsidc.org). Grey bars indicate cooling events as indicated in Greenland ice cores and terrestrial proxies from core SL152. 11.2, 11.2 ka event; PB, preboreal oscillation; GS 1/YD, Greenland stadial 1/Younger Dryas; GI, Greenland interstadial; Oldst. D., Oldest Dryas; H1, Heinrich event 1. This figure is available in colour online at wileyonlinelibrary.com.

Marine proxies

Dinocysts

During the late Pleniglacial, particularly between ca. 18 and ca. 16 cal ka BP, *Nematosphaeropsis labyrinthus* dominates the dinocyst assemblages with relative abundances approaching 50% (Fig. 3). Besides being a euryhaline species (Marret and Zonneveld, 2003; Pross *et al.*, 2004), this taxon generally indicates cool surface waters (e.g. Sangiorgi *et al.*, 2002). Similarly, *Spiniferites elongatus* also represents a cool-water indicator (Harland, 1983; Combourieu-Nebout *et al.*, 1998; Marret and Zonneveld, 2003; Marino *et al.*, 2009). Relatively high (>4%) percentages of *S. elongatus* occur between 17.5 and 16 cal ka BP (Fig. 3), and the combined percentages of the cold-water indicators *N. labyrinthus* and *S. elongatus* are highest at ca. 16.5 cal ka BP (Fig. 5D). A short-lived peak of *Lingulodinium machaerophorum* and *Operculodinium centrocarpum* precedes the broader maximum of cold-water indicators at ca. 19 cal ka BP.

Tectatodinium psilatum and *Spiniferites cruciformis* (results for the latter are not shown here) occur rarely, but consistently since 19 cal ka BP. This indicates that these species can probably not be used as an indicator for a connection between the Aegean and the Black Sea as previously suggested by Aksu *et al.* (1995). This is because, in light of glacial sea-level dynamics, a linkage of the Aegean Sea and the Black Sea cannot have been established prior to a strong sea-level rise

above 'glacial' values, probably not earlier than ca. 10–9 cal ka BP (Aksu *et al.*, 1995; Major *et al.*, 2006; Bahr *et al.*, 2008) or even later (e.g. Sperling *et al.*, 2003).

After ca. 16 cal ka BP, the percentages of cold-water indicators, in particular *N. labyrinthus*, decline, while percentages of the salinity-tolerant taxon *O. centrocarpum* (Combourieu-Nebout *et al.*, 1998; Marret and Zonneveld, 2003) reach peak values at ca. 15.4 cal ka BP. During the Bølling and Allerød, between ca. 14.6 and 12.7 cal ka BP, *Spiniferites* species dominate the dinocyst assemblages. This interval is furthermore characterised by repeated increases in *S. elongatus* percentages. Heterotrophic taxa (consisting mainly of *Brigantedinium* spp.) show several pronounced peaks at the onset of the Bølling interstadial (ca. 14.5 cal ka BP) and during the Allerød interstadial (between ca. 14 and ca. 13 cal ka BP).

The YD (ca. 12.6 to ca. 11.7 cal ka BP) is characterised by an increase of cold-water indicators at the expense of total *Spiniferites*, *Bitectatodinium tepikiense* and heterotrophic species (Figs 2 and 3). Notably, *N. labyrinthus* percentages reach maximum values at ca. 12.3 cal ka BP, whereas *S. elongatus* is abundant during the onset (ca. 12.7 to 12.4 cal ka BP) and the end of the YD (ca. 12.0 to 11.8 cal ka BP).

Between 11.2 and 10.2 cal ka BP, following a short-term percentage increase of *Spiniferites* species, *L. machaerophorum* dominates the dinocyst assemblages. This taxon indicates estuarine to neritic conditions and occurs under conditions of enhanced sea-surface productivity (e.g. Wall *et al.*, 1977;

Combourieu-Nebout et al., 1998; Marret and Zonneveld, 2003). The subsequent phase is characterised by a decrease in L. machaerophorum percentages and a coeval dominance of Operculodinium spp.

With the onset of S1 formation, percentages of Operculodinium spp. rapidly decrease. A transition from high N. labyrinthus percentages over high percentages of L. machaerophorum to increased O. centrocarpum percentages preceding S1 formation has previously been described from the northern Aegean Sea (Aksu et al., 1995); a rapid increase of O. centrocarpum percentages directly preceding S1 formation is also known from the Adriatic Sea (Combourieu-Nebout et al., 1998). Hence we suggest that this sequence of dominant taxa may be characteristic for the Aegean and Adriatic seas, and that the last percentage peak of N. labyrinthus preceding S1 may be used as a biostratigraphic marker for the YD, similar to high percentages in Artemisia and Chenopodiaceae in the terrestrial realm (Rossignol-Strick, 1995; Kotthoff et al., 2008a). After 9.3 cal ka BP, O. centrocarpum percentages recover (>36%), and Operculodinium spp. remain the most abundant cysts apart from Spiniferites spp. during the first phase of S1 (Fig. 3). Cysts of heterotrophic taxa reach maximum percentages during S1 deposition (Fig. 3).

Planktic foraminiferal oxygen isotopes from core SL152

As described above, the $\delta^{18}O$ record of core SL152 is partly based on G. ruber for the interval from ca. 17 to ca. 13 cal ka BP and supplemented by data from N. incompta. Besides a single, very low value at the beginning of the late Pleniglacial, the $\delta^{18}O_{ruber}$ record between the late Pleniglacial and the earliest Holocene shows highly positive values ($\sim$2‰) indicative of colder and/or more saline summer surface waters (Fig. 5C). Between ca. 11.5 and ca. 10.5 cal ka BP, $\delta^{18}O_{ruber}$ decreases, with the lowest values recorded during S1 deposition. This observation is in agreement with previous studies from the Aegean Sea (Casford et al., 2002, 2003; Marino et al., 2009). The $\delta^{18}O_{pachyderma}$ values for the Lateglacial show even heavier values, with a marked decrease ($\sim$1‰) during the Allerød and Bølling interstadials. The combined curves are generally similar to the planktic $\delta^{18}O$ record from neighbouring core SL148 (Fig. 5C; Kuhnt et al., 2007).

Planktic foraminiferal assemblages from core SL 148

During most of the study interval, cold-water indicators N. incompta and T. quinqueloba dominate the planktic foraminiferal fauna, making up to 80% of the entire assemblage between 19 and 12 cal ka BP (Fig. 5B). T. quinqueloba is very abundant during most of the late Pleniglacial between $\sim$19 and $\sim$16.2 cal ka BP, the YD interval (ca. 12.6 to ca. 11.7 cal ka BP) and the onset of S1 formation at ca. 9.5 cal ka BP. At the end of the late Pleniglacial, N. incompta becomes the dominant faunal element (>50%) and remains abundant until the onset of the YD. Percentages of cold indicator N. pachyderma >1% occur at ca. 17.4 and ca. 16.5 cal ka BP.

From ca. 12 cal ka BP onwards, warm-water taxa including among others G. ruber (pink and white) and G. sacculifer, show a continuous abundance increase, with a peak at ca. 10 cal ka BP, where they make up 50% of the assemblage. This rise in the abundance of warm-water taxa is also paralleled by an increase of temperate forms (predominantly Globigerina bulloides).

Synthesis of marine and terrestrial signals

Late Pleniglacial (ca. 19 to ca. 14.7 cal ka BP)

As suggested by the pollen-based climate reconstructions from core SL152, the late Pleniglacial in the northern borderlands of the Aegean Sea is characterised by cold and dry climate conditions. This interval is punctuated by an interlude of particularly dry and cold conditions between ca. 17.3 and ca. 16.3 cal ka BP. The strong percentage increase of dinocyst cold indicators starting at ca. 19 cal ka BP (Fig. 5D), especially N. labyrinthus (Fig. 3), suggests decreasing sea surface temperature (SST) during that time, culminating in particularly cold conditions at ca. 16.5 cal ka BP. High relative abundances of T. quinqueloba and a subordinate peak of N. pachyderma in core SL148 also indicate lower SSTs at ca. 16.5 cal ka BP (Fig. 5B), as do high $\delta^{18}O$ values (Fig. 5).

This particularly cold phase around ca. 16.5 cal ka BP is coeval with an interval of harsh climate conditions, as observed in other sectors along the southern European margin (e.g. Combourieu-Nebout et al., 1998, 2009; Kageyama et al., 2005; Brauer et al., 2007; Fletcher and Sánchez Goñi, 2008) and Asia Minor (e.g. Fleitmann et al., 2009). It appears to be linked to the H1 event in the northern North Atlantic Ocean (e.g. Bond et al., 1993). Hence the reduction of oceanic heat transport to the high northern latitudes as connected to Heinrich events (e.g. Bond et al., 1993) also led to significantly dryer/colder conditions in the eastern Mediterranean region. A possible link within this teleconnection could be sought in a transient strengthening of the Siberian High during H1, resulting in harsher conditions during the winter and early spring months. A similar mechanism has already been shown for cold spells in the Aegean region during the Holocene (e.g. Rohling et al., 2002; Kotthoff et al., 2008b), and for changes in Recent climate of the eastern Mediterranean region (Saaroni et al., 1996).

After the particularly cool conditions at ca. 16.5 cal ka BP, the decrease of N. labyrinthus percentages and the subsequent increases of O. centrocarpum, Lingulodinium machaerophorum and Spiniferites spp. percentages between ca. 16 and ca. 14.3 cal ka BP are probably caused by enhanced freshwater/nutrient influx and increasing surface-water temperatures due to a climatic amelioration. This view is supported by rapid relative abundance increases of benthic foraminiferal high-food/low-O_2 indicators and N. incompta in core SL148 (Fig. 5). As previously suggested by Rohling et al. (1993) and Casford et al. (2002), an increased abundance of N. incompta may indicate prolonged, intensified surface-water stratification and a more pronounced deep chlorophyll maximum in summer.

During the same interval (between ca. 16 and ca. 14.5 cal ka BP), the borderlands of the Aegean Sea witnessed the coeval spreading of broad-leaved trees (indicated by increasing NSAP percentages) and a decrease of steppe vegetation (Fig. 5E). Quantitative pollen-based climate reconstructions show an MP_{year} increase in the borderlands of the Aegean Sea between ca. 16 and ca. 14.5 cal ka BP (Fig. 5G); MT_{year} became slightly milder between ca. 15.5 and 15.1 cal ka BP (Fig. 5F). Such a climatic amelioration is compatible with increased melting rates of glaciers in the Rhodope mountains during that time, as suggested by Ehrmann et al. (2007).

Our data suggest a further climate setback in the borderlands of the Aegean Sea at ca. 15 cal ka BP, which is probably equivalent to the Oldest Dryas (Fig. 5F and G). A comparable setback is also reflected in the stalagmite $\delta^{18}O$ records from the Sofular Cave (Turkey; Fleitmann et al., 2009) and from the Hula Cave (Asia; e.g. Wang et al., 2001), and furthermore in the NGRIP $\delta^{18}O$ data (Svensson et al., 2008) and, to a lesser degree, in the GISP2 $\delta^{18}O$ record (Stuiver and Grootes, 2000; Fig. 5H). Although H1 is dated between ca. 16.5 and ca. 16 cal ka BP (Bond et al., 1993), several authors imply that this setback may still be related to H1 (e.g. Svensson et al., 2008; Fleitmann et al., 2009).

Following this interpretation, the H1 in the Aegean region can be characterised as a ca. 2.4 ka long interval (ca. 17.4 to ca.

15 cal ka BP) that comprises a particularly dry and cold phase at ca. 16.5 cal ka and a milder phase between ca. 15.7 and ca. 15.1 cal ka BP. A comparison with terrestrial H1 signals in the borderlands of the western Mediterranean Sea and in Italy, where the H1 is reflected in strong increases of SEP (e.g. an *Artemisia* pollen percentage increase of >20%; Brauer *et al.*, 2007; Fletcher and Sánchez Goñi, 2008; Combourieu-Nebout *et al.*, 2009) and an MT_{year} decline of >5°C (with temperature of the coldest month decreasing by ~3°C; Kageyama *et al.*, 2005), shows that the impact of the H1 was less pronounced in the Aegean region compared to preceding climate conditions. In the central Mediterranean region, the impact of the H1 on vegetation dynamics was probably stronger than in the Aegean region, but weaker than in the borderlands of the western Mediterranean Sea (Combourieu-Nebout *et al.*, 1998). This W–E gradient during H1 can be ascribed to the generally dryer and colder conditions in the eastern Mediterranean region prior to H1 as compared to the milder conditions in the western Mediterranean region (e.g. Fletcher and Sánchez Goñi, 2008; Combourieu-Nebout *et al.*, 2009; see also below).

Bølling–Allerød interstadial (ca. 14.7 to ca. 12.6 cal ka BP)

Our pollen-based vegetation data and quantitative climate reconstructions for the terrestrial realm as derived from core SL152 suggest relatively mild conditions during Bølling and Allerød in the northern Aegean borderlands, with MT_{year} even reaching Holocene values. However, a pronounced climate setback at ca. 13.8 ka, which – depending on terminology – represents the local equivalent of the Older Dryas/Greenland stadial 1d (e.g. Lowe *et al.*, 2008; Dormoy *et al.*, 2009) and of the Oldest Dryas in records from western Europe (e.g. Litt *et al.*, 2001; ca. 13.8 cal ka BP), separates the relatively stable Bølling (GI-1e) from the more unstable Allerød (GI 1c–1a). Low SSTs during this setback are indicated by high percentages of dinocyst cold indicators (especially *S. elongatus*). In the terrestrial realm, this interval is characterised by decreases in NSAP percentages, MT_{year} and MP_{year} (Fig. 5E–G).

Rather unstable climate conditions during the following Allerød are indicated for the borderlands of the Aegean Sea by repeated oscillations in the NSAP percentages, and concomitant MT_{year} and MP_{year} setbacks (Fig. 5E–G). For the marine realm, coeval setbacks are documented by short increases of the cold-water indicator *S. elongatus* (Fig. 3), while particularly low values of *N. labyrinthus* and the first consistent occurrences of *Impagidinium* species indicate generally warmer conditions (e.g. Combourieu-Nebout *et al.*, 1998; Sangiorgi *et al.*, 2003) during the Allerød (Fig. 3).

Heterotrophic dinocysts occur repeatedly during the Bølling and the more humid phases of the Allerød, with percentages almost comparable with those reached during S1 (Fig. 3). They probably indicate an enhanced nutrient supply. This view is supported by a strong percentage increase of intermediate to deep infaunal benthic foraminifers in core SL148, which implies an enhanced nutrient supply to the seafloor (Kuhnt *et al.*, 2007; Fig. 5A). The last more humid phase of the Allerød (ca. 13.2 to 12.7 cal ka BP) is characterised by a decrease in foraminifer high-productivity indicators (Fig. 5) and a coeval increase in foraminifer and dinocyst cold indicators, and SEP, reflecting the rapid transition to the YD.

Younger Dryas (ca. 12.6 to ca. 11.7 cal ka BP)

Our dinocyst cold-water indicators and the cold-water species *T. quinqueloba* show a marked abundance increase with the onset of the YD (Fig. 5B and D). Apart from surface-water cooling, the increase of *T. quinqueloba* may also be ascribed to

enhanced input of terrestrial material and a consequent increase in turbidity, since the asymbiotic form of *T. quinqueloba* has been discussed as indicative of turbid water bodies off California, up to 100 km offshore (Ortiz *et al.*, 1995).

Our pollen-based quantitative climate data indicate an abrupt MP_{year} drop between ca. 12.8 and ca. 12.7 cal ka BP, while MT_{year} started declining slightly earlier (~12.9 cal ka BP), and more gradually; lowest MT_{year} were only reached at 12.5 cal ka BP (Fig. 5F and G). Two particularly dry phases of the YD are indicated by especially high SEP percentages and low MP_{year} values at ca. 12.6 and ca. 11.8 cal ka BP.

Our results support and complement the findings of Rossignol-Strick (1995), Kuhnt *et al.* (2007), Kotthoff *et al.* (2008a) and Dormoy *et al.* (2009) that the YD is very strongly reflected in the Aegean region, and its impact on both the marine and the terrestrial realm was abrupt, with a decline of annual temperature by 6°C and an annual precipitation decrease of 300 mm (50%), the latter occurring abruptly within ca. 150 a only. This is different from findings from more westerly settings of the Mediterranean region: in the Adriatic Sea, the YD is reflected in a less pronounced, shorter increase in *N. labyrinthus* percentages (Combourieu-Nebout *et al.*, 1998; Sangiorgi *et al.*, 2002) as compared to the northern Aegean Sea. Similarly, a milder YD in terrestrial environments of the central Mediterranean region is indicated by pollen records from Italy (e.g. Magny *et al.*, 2006; Brauer *et al.*, 2007) and western Greece (e.g. Lawson *et al.*, 2004, 2005). We ascribe this discrepancy to the generally milder temperatures during the YD in that region in comparison to the Aegean region. In terrestrial settings of the western Mediterranean region, the YD is expressed by the spreading of steppe elements, but temperature declines were also weaker than in the Aegean region (Fletcher and Sánchez Goñi, 2008; Combourieu-Nebout *et al.*, 2009; Dormoy *et al.*, 2009).

It cannot be excluded, however, that the abruptness and intensity of the terrestrial, pollen-based YD signal in the northern Aegean region are partly caused by changes in wind direction and intensity (Kotthoff *et al.*, 2008a); such a scenario has been reported from other regions in Europe (e.g. Brauer *et al.*, 2008) and is also suggested for the northern Aegean region (Ehrmann *et al.*, 2007). Increased storminess during the spring months could have been caused by abrupt changes in intensity and/or direction of the westerlies (Brauer *et al.*, 2008) and/or by a strengthening of the Siberian High (e.g. Rohling *et al.*, 2002; see also above).

Early Holocene (ca. 11.7 to ca. 9.6 cal ka BP)

Subsequent to the YD, the abundances of tropic–subtropic and transitional planktic foraminifers increase until ca. 10 cal ka BP, indicating a rise in SSTs (Fig. 5B). The planktic $\delta^{18}O$ records of the cores SL152 and SL148 (Fig. 5C; Kuhnt *et al.*, 2007) reflect the transition from glacial to interglacial conditions at ca. 11 cal ka BP, exemplified by a shift of ~2‰ towards lighter values.

For the terrestrial realm, the pollen-based quantitative climate data indicate a return to higher MT_{year} (>13°C) after the YD within ~150 a, while the MP_{year} appears to have increased more gradually. Both climate parameters underwent several oscillations, the strongest of which is registered at ca. 11 cal ka BP (Fig. 5). This setback is probably related to the '11.2 cal ka event' described from central Europe and the Mediterranean area (Hoek and Bos, 2007; Magny *et al.*, 2007; Dormoy *et al.*, 2009).

Subsequently, at ca. 10.5 cal ka BP, *L. machaerophorum* became the most frequent dinocyst taxon (Fig. 3). Its abundance increase points either to decreasing salinity or enhanced

nutrient input (e.g. Aksu *et al.*, 1995) and can probably be ascribed to increased meltwater input into the Aegean Sea due to the melting of glaciers in the Rhodope mountains, which resulted from the general temperature increase after the YD (Ehrmann *et al.*, 2007).

The following spreading of *Operculodinium* species between ca. 10.5 ka and 9.6 cal ka BP and the almost coeval increase of benthic foraminiferal high-food/low-O_2 indicators (Fig. 4; Kuhnt *et al.*, 2007) were probably caused by the onset of water column stratification due to increased precipitation. Such a precipitation increase is reflected by a rise in NSAP and the pollen-based quantitative MP_{year} reconstruction (Fig. 5E and H; Kotthoff *et al.*, 2008b). The increased MP_{year} and water stratification finally resulted in the formation of sapropel S1 in the northern Aegean Sea starting at ca. 9.6 cal ka BP (Kotthoff *et al.*, 2008b). The increase of *T. quinqueloba* percentages between ca. 10 and ca. 9.5 cal ka BP was probably not caused by decreasing temperature (Ortiz *et al.*, 1995), given that coeval increases in the percentages of dinocyst cold indicators are not observed (Fig. 3), and quantitative MT_{year} reconstructions for the terrestrial realm (Fig. 5F) suggest rather stable conditions. The onset of the *T. quinqueloba* increase, a taxon considered to be fairly tolerant towards lower salinities (Rohling *et al.*, 1993, 1997), is however, coeval with very high MP_{year} in the borderlands of the Aegean Sea (Fig. 5B and G). This observation implies that the *T. quinqueloba* increase was caused by increased freshwater input rather than declining temperatures.

Conclusions

To elucidate the response of terrestrial and marine ecosystems in the Aegean region to late Pleniglacial and Lateglacial climate perturbations, and to compare the impact of the H1 event with that of the YD, we have analysed and integrated marine and continental proxy data from two northern Aegean sediment cores in centennial-scale (125–400 a) resolution.

Our results allow clear identification of the impact of the H1 event on surface-water conditions and terrestrial ecosystems. Enhancing the already dry and cold conditions of the regional climate during the late Pleniglacial, the H1 event led to an additional decline in SST in the northern Aegean Sea and an MP_{year} and MT_{year} decrease in the borderlands of the Aegean Sea.

The Bølling and the Allerød were intervals of generally warmer and more humid climate in the northern Aegean region. The humid conditions led to increased runoff and nutrient input into the Aegean Sea. MT_{year} reached almost Holocene levels during both interstadials. However, several short-term climate setbacks (particularly the Older Dryas; ca. 13.8 cal ka BP) led to transient temperature decreases in the Aegean Sea and its borderlands; the borderlands further witnessed a decline in MP_{year}.

Climate conditions during the H1 and the YD were almost identical, with only slightly lower temperatures during the YD observed in the terrestrial realm. Similar dinocyst assemblages indicate comparable surface-water conditions in the northern Aegean Sea during both intervals. The YD, however, interrupted a transition to warmer and more humid conditions initiated during the Bølling/Allerød. The MT_{year} in the borderlands of the Aegean Sea declined by >6°C with the onset of the YD, and MP_{year} dropped by almost 50% within 150 mm. Therefore the YD witnessed strong changes in both marine and terrestrial ecosystems, while only slight ecological changes occurred during the H1, especially concerning the terrestrial realm and the foraminiferal assemblages.

The early Holocene until ca. 9 cal ka BP was characterised by relatively stable, high temperatures both in the marine and terrestrial realms, while MP_{year} in the borderlands gradually increased until the deposition of sapropel S1. A major climate setback at ca. 11 cal ka BP, probably correlative to a cold event at ca. 11.2 cal ka BP known from various European climate archives, strongly affected the terrestrial ecosystems. For the time interval from ca. 11.6 to ca. 9.6 cal ka BP, dinocyst assemblages reflect a transition to a stratified water column, increased nutrient input and higher SSTs in the marine realm of the Aegean region.

Abbreviations. C_{org}, organic carbon; H1, Heinrich 1 (event); MAT, modern analogue technique; MP_{year}, mean annual precipitation; MT_{year}, mean annual temperature; SST, sea surface temperature; YD, Younger Dryas.

References

Aksu AE, Yaşar D, Mudie PJ, *et al.* 1995. Late glacial–Holocene paleoclimatic and paleoceanographic evolution of the Aegean Sea: micropaleontological and stable isotopic evidence. *Marine Micropaleontology* **25**: 1–28.

Bahr A, Lamy F, Arz HW, *et al.* 2008. Abrupt changes of temperature and water chemistry in the late Pleistocene and early Holocene Black Sea. *Geochemistry, Geophysics, Geosystems* **9**: 1–16.

Barker S, Diz P, Vautravers MJ, *et al.* 2009. Interhemispheric Atlantic seesaw response during the last deglaciation. *Nature* **457**: 1097–1102.

Bé AWH, Tolderlund DS. 1971. Distribution and ecology of living planktonic foraminifera in surface waters of the Atlantic and Indian oceans. In: Funnell BW, Riedel WR editors. *The Micropalaeontology of Oceans*. Cambridge University Press: Cambridge, UK; 105–149.

Berger AL, Loutre MF. 1991. Insolation values for the climate of the last 10 million years. *Quaternary Science Reviews* **10**: 297–317.

Björck S, Walker MJC, Cwynar LC, *et al.* 1998. An event stratigraphy for the Last Termination in the north Atlantic region based on the Greenland ice-core record: a proposal by the INTIMATE group. *Journal of Quaternary Science* **13**: 283–292.

Bond G, Broecker W, Johnsen S, *et al.* 1993. Correlations between climate records from North Atlantic sediments and Greenland ice. *Nature* **365**: 143–147.

Bordon A, Peyron O, Lézine A-M, *et al.* 2009. Pollen-inferred Late-Glacial and Holocene climate in southern Balkans (Lake Maliq). *Quaternary International* **200**: 19–30.

Brauer A, Allen JRM, Mingram J, *et al.* 2007. Evidence for last interglacial chronology and environmental change from Southern Europe. *Proceedings of the National Academy of Sciences USA* **104**: 450–455.

Brauer A, Haug GH, Dulski P, *et al.* 2008. An abrupt wind shift in Western Europe at the onset of the Younger Dryas cold period. *Nature Geoscience* **1**: 520–523.

Broecker WS. 2000. Abrupt climate change: causal constraints provided by paleoclimate record. *Earth-Science Reviews* **51**: 137–154.

Broecker WS. 2006. Was the Younger Dryas triggered by a Flood? *Science* **312**: 1146–1148.

Cacho I, Grimalt JO, Pelejero C, *et al.* 1999. Dansgaard-Oeschger and Heinrich events imprints in Alboran Sea paleotemperatures. *Paleoceanography* **14**: 698–705.

Casford JSL, Rohling EJ, Abu-Zied R, *et al.* 2002. Circulation changes and nutrient concentrations in the late Quaternary Aegean Sea:

a nonsteady state concept for sapropel formation. *Paleoceanography* **17**. DOI: 10.1029/2000PA000601.

Casford JSL, Rohling EJ, Abu-Zied RH, *et al.* 2003. A dynamic concept for eastern Mediterranean circulation and oxygenation during sapropel formation. *Palaeogeography, Palaeoclimatology, Palaeoecology* **190**: 103–119.

Çatağay MN, Görür N, Algan O, *et al.* 2000. Late glacial–Holocene palaeoceanography of the Sea of Marmara; timing of connections with the Mediterranean and the Black seas. *Marine Geology* **167**: 191–206.

Chester R, Baxter GG, Behairy AKA, *et al.* 1977. Soil-sized eolian dusts from the lower troposphere of the Eastern Mediterranean Sea. *Marine Geology* **24**: 201–217.

Combourieu-Nebout N, Paterne M, Turon J-L, *et al.* 1998. A high-resolution record of the last deglaciation in the central Mediterranean Sea: palaeovegetation and palaeohydrological evolution. *Quaternary Science Reviews* **17**: 303–317.

Combourieu-Nebout N, Peyron O, Dormoy I, *et al.* 2009. Rapid climatic variability in the west Mediterranean during the last 25 000 years from high resolution pollen data. *Climate of the Past* **5**: 503–521.

Cramp A, Collins M, West R. 1988. Late Pleistocene–Holocene sedimentation in the NW Aegean Sea: a palaeoclimatic palaeoceanographic reconstruction. *Palaeogeography, Palaeoclimatology, Palaeoecology* **68**: 61–71.

Darling KF, Kucera M, Kroon D, *et al.* 2006. A resolution for the coiling direction paradox in *Neogloboquadrina pachyderma*. *Paleoceanography* **21**: PA2011.

Dormoy I, Peyron O, Combourieu-Nebout N, *et al.* 2009. Terrestrial climate variability and seasonality changes in the Mediterranean region between 15 000 and 4000 years BP deduced from marine pollen records. *Climate of the Past* **5**: 615–632.

Ehrmann W, Schmiedl G, Hamann Y, *et al.* 2007. Distribution of clay minerals in surface sediments of the Aegean Sea: a compilation. *International Journal of Earth Sciences* **96**: 769–780.

Fairbanks RG, Mortlock RA, Chiu T-C, *et al.* 2005. Radiocarbon calibration curve spanning 0 to 50,000 years BP based on paired ^{230}Th/^{234}U and ^{14}C dates on pristine corals. *Quaternary Science Reviews* **24**: 1781–1796.

Fleitmann D, Cheng H, Badertscher S, *et al.* 2009. Timing and climatic impact of Greenland interstadials recorded in stalagmites from northern Turkey. *Geophysical Research Letters* **36**: L19707.

Fletcher WJ, Sánchez Goñi MF. 2008. Orbital and sub-orbital-scale climate impacts on vegetation of the western Mediterranean basin over the last 48,000 yr. *Quaternary Research* **70**: 451–464.

Guiot J. 1990. Methodology of palaeoclimatic reconstruction from pollen in France: *Palaeogeography. Palaeoclimatology, Palaeoecology* **80**: 49–69.

Hamann Y, Ehrmann W, Schmiedl G, *et al.* 2008. Sedimentation processes in the Eastern Mediterranean Sea during the Late Glacial and Holocene revealed by end-member modelling of the terrigenous fraction in marine sediments. *Marine Geology* **248**: 97–114.

Harland R. 1983. Distribution map of recent dinoflagellate cysts in bottom sediments from the North Atlantic Ocean and adjacent seas. *Palaeontology* **16**: 321–387.

Hayes A, Kucera M, Kallel N, *et al.* 2005. Glacial Mediterranean sea surface temperatures based on planktonic foraminiferal assemblages. *Quaternary Science Reviews* **24**: 999–1016.

Hemleben C, Spindler M, Anderson OR. 1989. *Modern Planktonic Foraminifera*. Springer: Berlin.

Hilbrecht H. 1996. *Extant planktic foraminifera and the physical environment in the Atlantic and Indian Oceans*. Mitteilungen aus dem Geologischen Institut der Eidgen. Technischen Hochschule und der Universität Zürich, Neue Folge. No. 300, Zürich.

Hilbrecht H. 1997. Morphologic gradation and ecology in *Neogloboquadrina pachyderma* and *N. dutertrei* (planktic foraminifera) from core top sediments. *Marine Micropaleontology* **31**: 31–43.

Hoek WZ, Bos JAA. 2007. Early Holocene climate oscillations: causes and consequences. *Quaternary Science Reviews* **26**: 1901–1906.

Kageyama M, Combourieu Nebout N, Sepulchre P, *et al.* 2005. The Last Glacial Maximum and Heinrich Event 1 in terms of climate and vegetation around the Alboran Sea: a preliminary model-data comparison. *Comptes Rendus Geoscience* **337**: 983–992.

Kotthoff U, Müller UC, Pross J, *et al.* 2008a. Late Glacial and Holocene vegetation dynamics in the Aegean region: an integrated view based on pollen data from marine and terrestrial archives. *The Holocene* **18**: 1019–1032.

Kotthoff U, Pross J, Müller UC, *et al.* 2008b. Climate dynamics in the borderlands of the Aegean Sea during deposition of Sapropel S1 deduced from a marine pollen record. *Quaternary Science Reviews* **27**: 832–845.

Kucera M. 2007. Planktonic foraminifera as tracers of past oceanic environments. In: Hillaire-Marcel C, De Vernal A editors. *Proxies in Late Cenozoic Paleoceanography*. Elsevier: Amsterdam; 213–262.

Kuhnt T, Schmiedl G, Ehrmann W, *et al.* 2007. Deep-sea ecosystem variability of the Aegean Sea during the past 22 kyr as revealed by benthic foraminifera. *Marine Micropaleontology* **64**: 141–162.

Lane-Serff GF, Rohling EJ, Bryden HL, *et al.* 1997. Postglacial connection of the Black Sea to the Mediterranean and its relation to the timing of sapropel formation. *Paleoceanography* **12**: 169–174.

Lawson IT, Frogley M, Bryant C, *et al.* 2004. The Lateglacial and Holocene environmental history of the Ioannina basin, north-west Greece. *Quaternary Science Reviews* **23**: 1599–1625.

Lawson IT, Al-Omari S, Tzedakis PC, *et al.* 2005. Lateglacial and Holocene vegetation history at Nisi Fen and the Boras mountains, northern Greece. *The Holocene* **15**: 873–887.

Litt T, Brauer A, Goslar T, *et al.* 2001. Correlation and synchronisation of Lateglacial continental sequences in northern central Europe based on annually laminated lacustrine sediments. *Quaternary Science Reviews* **20**: 1233–1249.

Lowe JJ, Rasmussen SO, Björck S, *et al.* the INTIMATE group. 2008. Synchronisation of palaeoenvironmental events in the North Atlantic region during the Last Termination: a revised protocol recommended by the INTIMATE group. *Quaternary Science Reviews* **27**: 6–17.

Lykousis V, Chronis G, Tselepides A, *et al.* 2002. Major outputs of the recent multidisciplinary biogeochemical researches undertaken in the Aegean Sea. *Journal of Marine Systems* **33–34**: 313–334.

Magny M, de Beaulieu J-L, Drescher-Schneider R, *et al.* 2006. Climatic oscillations in central Italy during the Last Glacial–Holocene transition: the record from Lake Accesa. *Journal of Quaternary Science* **21**: 311–320.

Magny M, Vannière B, de Beaulieu J-L, *et al.* 2007. Early-Holocene climatic oscillations recorded by lake-level fluctuations in west-central Europe and in central Italy. *Quaternary Science Reviews* **26**: 1951–1964.

Major CO, Goldstein SL, Ryan WBF, *et al.* 2006. The co-evolution of Black Sea level and composition through the last deglaciation and its paleoclimatic significance. *Quaternary Science Reviews* **25**: 2031–2047.

Marino G, Rohling EJ, Rijpstra WI, *et al.* 2007. Aegean Sea as driver of hydrographic and ecological changes in the eastern Mediterranean. *Geology* **35**: 675–678.

Marino G, Rohling EJ, Sangiorgi F, *et al.* 2009. Early and middle Holocene in the Aegean Sea: interplay between high and low-latitude climate variability. *Quaternary Science Reviews* **28**: 3246–3262.

Marret F, Zonneveld KAF. 2003. Atlas of modern organic-walled dinoflagellate cyst distribution. *Review of Palaeobotany and Palynology* **125**: 1–200.

May PW. 1982. Climatological flux estimates in the Mediterranean Sea: Part 1. Winds and wind stresses. *Naval Ocean Research and Development Activity, Rep. 54* NSTL Station, MS.

McManus JF, Francois R, Gherardi J-M, *et al.* 2004. Collapse and rapid consumption of Atlantic meridional circulation linked to deglacial climate changes. *Nature* **428**: 834–837.

Mulitza S, Prange M, Stuut J-B, *et al.* 2008. Sahel megadroughts triggered by glacial slowdowns of Atlantic meridional overturning. *Paleoceanography* **23**: PA4206.

Ortiz JD, Mix AC, Collier RW. 1995. Environmental control of living symbiotic and asymbiotic foraminifera of the California Current. *Paleoceanography* **10**: 987–1009.

Perissoratis C, Conispoliatis N. 2003. The impacts of sea level changes during the latest Pleistocene and Holocene times on the morphology of Ionian and Aegean seas (SE Alpine Europe). *Marine Geology* **196**: 145–156.

Poulos SE, Drakopoulos PG, Collins MB. 1997. Seasonal variability in sea surface oceanographic conditions in the Aegean Sea (eastern Mediterranean): an overview. *Journal of Marine Systems* **13**: 225–244.

Pross J. 2001. Paleo-oxygenation in Tertiary epeiric seas: evidence from dinoflagellate cysts. *Palaeogeography, Palaeoclimatology, Palaeoecology* **166**: 369–381.

Pross J, Kotthoff U, Zonneveld KAF. 2004. Die Anwendung organisch-wandiger Dinoflagellatenzysten zur Rekonstruktion von Paläoumwelt, Paläoklima und Paläozeanographie: Möglichkeiten und Grenzen. *Paläontologische Zeitschrift* **78**: 5–39.

Pross J, Kotthoff U, Müller UC, *et al.* 2009. Massive perturbation in terrestrial ecosystems of the Eastern Mediterranean region associated with the 8.2 kyr climatic event. *Geology* **37**: 887–890.

Rohling EJ, Jorissen FJ, Vergnaud-Grazzini C, *et al.* 1993. Northern Levantine and Adriatic Quaternary planktic foraminifera: reconstruction of paleoenvironmental gradients. *Marine Micropaleontology* **21**: 191–218.

Rohling EJ, Jorissen FJ, De Stigter HC. 1997. A 200 year interruption of Holocene sapropel formation in the Adriatic Sea. *Journal of Micropaleontology* **16**: 97–108.

Rohling EJ, Mayewski PA, Abu-Zied RH, *et al.* 2002. Holocene atmosphere–ocean interactions: records from Greenland and the Aegean Sea. *Climate Dynamics* **18**: 587–593.

Rossignol-Strick M. 1995. Sea-land correlation of pollen records in the Eastern Mediterranean for the Glacial–Interglacial transition: biostratigraphy versus radiometric time-scale. *Quaternary Science Reviews* **14**: 893–915.

Rossignol-Strick M, Paterne M. 1999. A synthetic pollen record of the eastern Mediterranean sapropels of the last 1 Ma: implications for the time-scale and formation of sapropels. *Marine Geology* **153**: 221–237.

Saaroni H, Bitan A, Alpert P, *et al.* 1996. Continental polar outbreaks into the Levant and the Eastern Mediterranean. *International Journal of Climatology* **16**: 1175–1191.

Sánchez Goñi MF, Loutre MF, Crucifix M, *et al.* 2005. Increasing vegetation and climate gradient in Western Europe over the Last Glacial Inception (122–110 ka): model–data comparison. *Earth and Planetary Science Letters* **231**: 111–130.

Sangiorgi F, Capotondi L, Brinkhuis H. 2002. A centennial scale organic-walled dinoflagellate cyst record of the last deglaciation in the South Adriatic Sea (Central Mediterranean). *Palaeogeography, Palaeoclimatology, Palaeoecology* **186**: 199–216.

Sangiorgi F, Capotondi L, Combourieu-Nebout N, *et al.* 2003. Holocene seasonal sea-surface temperature variations in the southern Adriatic Sea inferred from a multiproxy approach. *Journal of Quaternary Science* **18**: 723–732.

Siani G, Paterne M, Michel E, *et al.* 2001. Mediterranean sea surface radiocarbon reservoir age changes since the Last Glacial Maximum. *Science* **294**: 1917–1920.

Sluijs A, Pross J, Brinkhuis H. 2005. From greenhouse to icehouse: organic-walled dinoflagellate cysts as paleoenvironmental indicators in the Paleogene. *Earth-Science Reviews* **68**: 281–315.

Sperling M, Schmiedl G, Hemleben C, *et al.* 2003. Black Sea impact on the formation of eastern Mediterranean sapropel S1? Evidence from the Marmara Sea. *Palaeogeography, Palaeoclimatology, Palaeoecology* **190**: 9–21.

Stuiver M, Grootes PM. 2000. GISP2 oxygen isotope ratios. *Quaternary Research* **53**: 277–284.

Svensson A, Andersen KK, Bigler M, *et al.* 2008. A 60 000 year Greenland stratigraphic ice core chronology. *Climate of the Past* **4**: 47–57.

Theocharis A, Nittis K, Kontoyiannis H, *et al.* 1999. Climatic changes in the Aegean Sea influence the Eastern Mediterranean thermohaline circulation (1986–1997). *Geophysical Research Letters* **26**: 1617–1620.

Verleye TJ, Mertens KN, Louwye S, *et al.* 2009. Holocene salinity changes in the southwestern Black Sea: a reconstruction based on dinoflagellate cysts. *Palynology* **33**: 77–100.

Wall D, Dale B, Lohmann GP, *et al.* 1977. The environment and climatic distribution of dinoflagellate cysts in modern marine sediments from regions in the north and south Atlantic oceans and adjacent seas. *Marine Micropaleontology* **2**: 121–200.

Wang YJ, Cheng H, Edwards RL, *et al.* 2001. A high-resolution absolute-dated late Pleistocene monsoon record from Hulu Cave, China. *Science* **294**: 2345–2348.

Waelbroeck C, Duplessy J-C, Michel E, *et al.* 2001. The timing of the last deglaciation in North Atlantic climate records. *Nature* **412**: 724–727.

Weldeab S, Lea DW, Schneider RR, *et al.* 2007. 155,000 years of West African Monsoon and ocean thermal evolution. *Science* **316**: 1303–1307.

Zonneveld KAF, Versteegh GJM, de Lange GJ. 2001. Palaeoproductivity and post-depositional aerobic organic matter decay reflected by dinoflagellate cyst assemblages of the Eastern Mediterranean S1 sapropel. *Marine Geology* **172**: 181–195.